

magnitude larger than in star-forming galaxies. This all suggests a heating source other than stars and the AGN is the obvious alternative. Differential magnification of AGN-heated gas therefore seems to be responsible for the high luminosity of the CO(9 → 8) line.

Although highly excited regions with CO emission amplified by gravitational lensing are good markers of the presence of molecular gas at high redshifts, they may give a poor representation of its average physical conditions, particularly of its total mass and distribution. At  $z > 3$ , this excitation bias becomes more serious since millimetre-wave interferometers, the instruments usually used for such searches, can detect only CO  $J + 1 \rightarrow J, J > 2$  whose excitation requirements are  $n(\text{H}_2) \geq 10^4 \text{ cm}^{-3}$  and  $T \geq 50 \text{ K}$ . These values, being typical of the average conditions in star-forming clouds, mark a gradual excitation turnover.

Observations of the CO(1 → 0) and CO(2 → 1) transitions, with their minimal excitation requirements, may reveal much larger molecular gas reservoirs at high redshifts. The VLA is currently the only instrument capable of sensitive, sub-arcsecond observations of these lines and will thus be an important tool for unbiased surveys of metal-enriched H<sub>2</sub> gas around objects in the distant Universe<sup>21</sup>. □

## Methods

Our observations took place during 23–24 April 2000 using the VLA in its C configuration. After all overheads, 20 hours were spent integrating on APM08279+5255. 19 of the 27 antennas were equipped with 43-GHz receivers ( $T_{\text{sys}} = 45\text{--}100 \text{ K}$ ); all were equipped with 22-GHz receivers, including eleven new receivers with  $T_{\text{sys}} \sim 40 \text{ K}$  (compared with 100–150 K for the remainder).

We used the new fast-switching technique<sup>22,23</sup>, recording data every 3.3 s, with 30 s on the calibrator and 170 s on the source (210 s in the 22-GHz band); the typical slewing overhead to the compact phase calibrator, 0824+558, 3.3° away was 7 s. The pointing accuracy was checked every hour.

This technique yields diffraction-limited images at the highest VLA operating frequencies over long baselines. Conventional phase referencing would not have been able to track tropospheric phase variations and self-calibration techniques could not be employed because of the low signal-to-noise ratio per baseline.

We used the continuum mode, placing emphasis on sensitivity rather than line profile information. A dual-polarization 50-MHz band was placed as close to the expected line centre as could be allowed by correlator limitations: 23.4649 GHz for CO  $J = 1 \rightarrow 0$  (+91 km s<sup>-1</sup> from the line centre<sup>3</sup>). Bandpass roll-off limited the effective bandwidth per intermediate frequency (IF) to ~45 MHz which, at  $z = 3.9$ , corresponds to  $\Delta v \sim 575 \text{ km s}^{-1}$  at 23 GHz. The remaining IF pair was tuned to simultaneously observe the continuum at 23.3649 GHz (+1,280 km s<sup>-1</sup>).

We obtained matching velocity coverage at 43 GHz (CO  $J = 2 \rightarrow 1$ ) by placing two contiguous 50-MHz dual-polarization bands at 46.9399 GHz (–20 km s<sup>-1</sup> from the line centre). The continuum was observed on a separate occasion with both IF pairs tuned to 43.3 GHz. The flux-density scale was fixed using 3C286; the uncertainty is ~15% at 23 GHz and ~20% at 46 GHz. Calibration and reduction of the data was standard in most respects and the r.m.s. noise in all the maps is similar to the expected theoretical limit.

We cannot completely rule out the possibility that phase errors—caused by atmospheric fluctuations too fast to be tracked even by our fast-switching scheme—are the cause of the extended CO emission, but we consider it to be remote. This is borne out by an extensive series of tests: inspection of the raw visibilities; separate imaging of left- and right-hand polarization maps; imaging of the most phase-stable subset of the data; and imaging of the calibrator source. The agreement between the nuclear CO  $J = 2 \rightarrow 1$  emission and its associated 3.5-cm continuum is also strong testimony to the coherence of the CO  $J = 2 \rightarrow 1$  map; the point-like 23.4-GHz continuum emission, observed simultaneously with the neighbouring line emission, provides similar supporting evidence for the resolved CO  $J = 1 \rightarrow 0$  emission.

Received 5 September; accepted 13 November 2000.

1. Telesco, C. M. Enhanced star formation and infrared emission in the centers of galaxies. *Annu. Rev. Astron. Astrophys.* **26**, 343–376 (1988).
2. Sanders, D. B., Scoville, N. Z. & Soifer, B. T. Molecular gas in luminous infrared galaxies. *Astrophys. J.* **370**, 158–171 (1991).
3. Downes, D., Neri, R., Wikind, T., Wilner, D. J. & Shaver, P. A. Detection of CO(4–3), CO(9–8), and dust emission in the broad absorption line quasar APM 08279+5255 at a redshift of 3.9. *Astrophys. J.* **513**, L1–L4 (1999).
4. Irwin, M. J., Ibata, R. A., Lewis, G. F. & Totten, E. J. APM 08279+5255: an ultraluminous broad absorption line quasar at a redshift  $z = 3.87$ . *Astrophys. J.* **505**, 529–535 (1998).
5. Lewis, G. F., Chapman, S. C., Ibata, R. A., Irwin, M. J. & Totten, E. J. Submillimeter observations of the ultraluminous broad absorption line quasar APM 08279+5255. *Astrophys. J.* **505**, L1–L5 (1998).
6. Ibata, R. A., Lewis, G. F., Irwin, M. J., Lehár, J. & Totten, E. J. NICMOS and VLA observations of the gravitationally lensed ultraluminous BAL quasar APM 08279+5255: detection of a third image. *Astron. J.* **118**, 1922–1930 (1999).

7. Egami, E. et al. APM 08279+5255: Keck near- and mid-infrared high-resolution imaging. *Astrophys. J.* **535**, 561–574 (2000).
8. Young, J. S. & Scoville, N. Z. Extragalactic CO—gas distributions which follow the light in IC 342 and NGC 6946. *Astrophys. J.* **258**, 467–489 (1982).
9. Young, J. S. & Scoville, N. Z. Molecular gas in galaxies. *Annu. Rev. Astron. Astrophys.* **29**, 581–625 (1991).
10. Dickman, R. L., Snell, R. L. & Schloerb, F. P. Carbon monoxide as an extragalactic mass tracer. *Astrophys. J.* **309**, 326–330 (1986).
11. Downes, D. & Solomon, P. M. Rotating nuclear rings and extreme starbursts in ultraluminous galaxies. *Astrophys. J.* **507**, 615–654 (1998).
12. Smail, I., Ivison, R. J. & Blain, A. W. A deep sub-millimeter survey of lensing clusters: a new window on galaxy formation and evolution. *Astrophys. J.* **490**, L5–L8 (1997).
13. Ivison, R. J. et al. An excess of submillimeter sources near 4C 41.17: a candidate proto-cluster at  $z = 3.8$ ? *Astrophys. J.* **542**, 27–34 (2000).
14. Papadopoulos, P. P. et al. CO(4–3) and dust emission in two powerful high- $z$  radio galaxies, and CO lines at high redshifts. *Astrophys. J.* **528**, 626–636 (2000).
15. Plume, R. et al. Large-scale <sup>13</sup>CO  $J = 5\text{--}4$  and [CI] mapping of Orion A. *Astrophys. J.* **539**, L133–L136 (2000).
16. Aalto, S., Booth, R. S., Black, J. H. & Johansson, L. E. B. Molecular gas in starburst galaxies: line intensities and physical conditions. *Astron. Astrophys.* **300**, 369–384 (1995).
17. Jackson, J. M., Paglione, T. A. D., Carlstrom, J. E. & Rieu, N. Submillimeter HCN and HCO+ emission from galaxies. *Astrophys. J.* **438**, 695–701 (1995).
18. Paglione, T. A. D., Jackson, J. M. & Ishizuki, S. The average properties of the dense molecular gas in galaxies. *Astrophys. J.* **484**, 656–663 (1997).
19. Papadopoulos, P. P. & Allen, M. L. Gas and dust in NGC 7469: submillimeter imaging and CO  $J = 3\text{--}2$ . *Astrophys. J.* **537**, 631–637 (2000).
20. Hughes, D. H., Gear, W. K. & Robson, E. I. The submillimetre structure of the starburst nucleus in M82—a diffraction-limited 450-micron map. *Mon. Not. R. Astron. Soc.* **270**, 641–649 (1994).
21. Ivison, R. J., Papadopoulos, P. P., Seaquist, E. R. & Eales, S. A. A search for molecular gas in a high-redshift radio galaxy. *Mon. Not. R. Astron. Soc.* **278**, 669–672 (1996).
22. Carilli, C. L. & Holdaway, M. A. Tropospheric phase calibration in millimeter interferometry. *Radio Sci.* **34**, 817–840 (1999).
23. Carilli, C. L., Menten, K. M. & Yun, M. S. Detection of CO(2–1) and radio continuum emission from the  $z = 4.4$  QSO BRI 1335–0417. *Astrophys. J.* **521**, L25–L28 (1999).

## Acknowledgements

P.P. and R.I. would like to thank E. Seaquist for early discussions and encouragement. We also thank R. Barvainis. The National Radio Astronomy Observatory is a facility of the National Science Foundation, operated under cooperative agreement by Associated Universities, Inc.

Correspondence and requests for materials should be addressed to R.I. (e-mail: rji@star.ucl.ac.uk).

## Substantial reservoirs of molecular hydrogen in the debris disks around young stars

W. F. Thi\*<sup>†</sup>, G. A. Blake<sup>‡</sup>, E. F. van Dishoeck\*<sup>§</sup>, G. J. van Zadelhoff\*<sup>¶</sup>, J. M. M. Horn<sup>‡</sup>, E. E. Becklin<sup>‡</sup>, V. Mannings<sup>§</sup>, A. I. Sargent<sup>||</sup>, M. E. van den Ancker<sup>¶</sup> & A. Natta<sup>#</sup>

\* Leiden Observatory, PO Box 9513, 2300 Leiden, The Netherlands

† Division of Geological and Planetary Sciences, Caltech 150–21,

§ SIRT Science Center, MS 314–6, Caltech, || Division of Physics,

Mathematics and Astronomy, Caltech 105–24, Pasadena, California 91125, USA

‡ Department of Physics and Astronomy, UCLA, California 90095–1562, USA

¶ Harvard Smithsonian Center for Astrophysics, 60 Garden Street, MS 42, Cambridge, Massachusetts 02138, USA

# Osservatorio Astrofisico di Arcetri, Largo E. Fermi 5, I-50125 Firenze, Italy

Circumstellar accretion disks transfer matter from molecular clouds to young stars and to the sites of planet formation. The disks observed around pre-main-sequence stars have properties consistent with those expected for the pre-solar nebula from which our own Solar System formed 4.5 Gyr ago<sup>1</sup>. But the ‘debris’ disks that encircle more than 15% of nearby main-sequence stars<sup>2–5</sup> appear to have very small amounts of gas, based on observations of the tracer molecule carbon monoxide<sup>6–8</sup>:

these observations have yielded gas/dust ratios much less than 0.1, whereas the interstellar value is about 100 (ref. 9). Here we report observations of the lowest rotational transitions of molecular hydrogen ( $H_2$ ) that reveal large quantities of gas in the debris disks around the stars  $\beta$  Pictoris, 49 Ceti and HD135344. The gas masses calculated from the data are several hundreds to a thousand times greater than those estimated from the CO observations, and yield gas/dust ratios of the same order as the interstellar value.

We used the Short Wavelength Spectrometer<sup>10</sup> (SWS) aboard the Infrared Space Observatory<sup>11</sup> (ISO), which provided the first opportunity to conduct measurements of the  $H_2$   $J = 2 \rightarrow 0$  S(0) 28  $\mu\text{m}$  and  $J = 3 \rightarrow 1$  S(1) 17  $\mu\text{m}$  pure rotational transitions above the Earth's atmosphere. These lines are the lowest energy transitions of the  $H_2$  molecule, but are difficult (17  $\mu\text{m}$ ) to impossible (28  $\mu\text{m}$ ) to observe from the ground because of telluric absorption. A number of classical T Tauri stars, Herbig Ae stars, and young (pre-)main-sequence stars with confirmed circumstellar disks were observed. The results of the searches toward T Tauri and Herbig Ae stars may be found elsewhere<sup>12,13</sup>. Here we focus on three sources previously classified as 'Vega type' objects; that is, low-mass disks with a dust population that is assumed to be dominated by second-generation grains<sup>3</sup>.

High-sensitivity mid-infrared observations of  $H_2$  such as those made possible by ISO have a number of advantages over more commonly used indirect tracers for assessing the molecular gas content of debris disks. For a gas of solar composition, molecular hydrogen is the overwhelmingly most abundant gaseous species (by four orders of magnitude), obviating the uncertainties associated with the conversion factors needed for other molecules.

The homonuclear nature of  $H_2$  makes the intrinsic pure rotational transition strengths sufficiently small that the optical depths of the mid-infrared lines are low, greatly simplifying the radiative transfer analysis. Because the lines appear in emission and are optically thin, any disk orientation can be studied. Substantially higher temperatures are required for excitation of the  $H_2$  vibration-rotation manifold near 2  $\mu\text{m}$ , and special geometries are needed to conduct either near-infrared or vacuum ultraviolet (electronic) absorption-line measurements. Thus, observations of the  $H_2$  mid-infrared lines are the most direct way of probing the bulk of the warm molecular gas in the inner  $\sim 100$  AU of disks.

The observed intensities of the  $H_2$  lines are close to the ISO sensitivity limit, as Fig. 1 shows, and so required the development of special software to supplement the standard SWS Interactive Analysis Package. A detailed description of the software used to improve the SWS dynamic range can be found elsewhere<sup>12,14</sup> (see Fig. 1 legend for details of the observing procedure). Table 1 presents the integrated line fluxes observed toward  $\beta$  Pictoris, 49 Ceti, and HD135344. The S(1)/S(0) ratios yield a direct measure of the excitation temperature provided the gas densities are large enough that collisional rates exceed ultraviolet pumping and spontaneous emission from the  $J = 2$  and 3 levels ( $n_{\text{cr}} \geq 10^4 \text{ cm}^{-3}$ ). For both the debris disks reported here and the disks surrounding T Tauri and Herbig Ae stars<sup>12</sup>, temperatures near 100 K are found—values comparable to the dust temperatures derived from fits of debris disk spectral energy distributions<sup>15</sup>. The non-detection of the  $J = 4 \rightarrow 2$  S(2) and  $J = 5 \rightarrow 3$  S(3) lines at 12.278 and 9.662  $\mu\text{m}$  limits the gas temperature to less than 250 K.

The total gas mass is very sensitive to temperature because the transition upper states lie at 510 and 1,015 K above ground, respectively, but, as outlined in Table 1, is straightforward to derive if thermal equilibrium is assumed and the distance to the source is known. Values range from a minimum of 0.17  $M_J$  (Jupiter mass) for  $\beta$  Pictoris to just over 6.6  $M_J$  for HD135344. Only an upper limit to the S(1) flux is available for 49 Ceti, which constrains the temperature at less than 100 K, corresponding to gas masses of at least 0.35  $M_J$ . The uncertainties in the inferred masses are estimated to be a factor of three, and stem mainly from the weakness of the lines and the unknown molecular hydrogen ortho/para ratio in such disks.

The line shapes are unresolved at the velocity resolution available to ISO, and 49 Ceti and HD135344 are too far away for their disks to be resolved with the large beams sampled by the SWS. Although  $\beta$  Pictoris is extended in the ISO-SWS beam, only observations centred on the star have been performed. As a result, no spatial information is available for the gas, and the fluxes obtained thus yield only lower limits for the gas mass.

Table 1 also lists the minimum dust masses derived from ISO measurements of the 60–240  $\mu\text{m}$  continuum fluxes by assuming the emitting particles are small compared to the observing wavelength<sup>15</sup> along with the gas mass estimated by CO observations. As can be seen, the gas mass exceeds that inferred for dust grains by

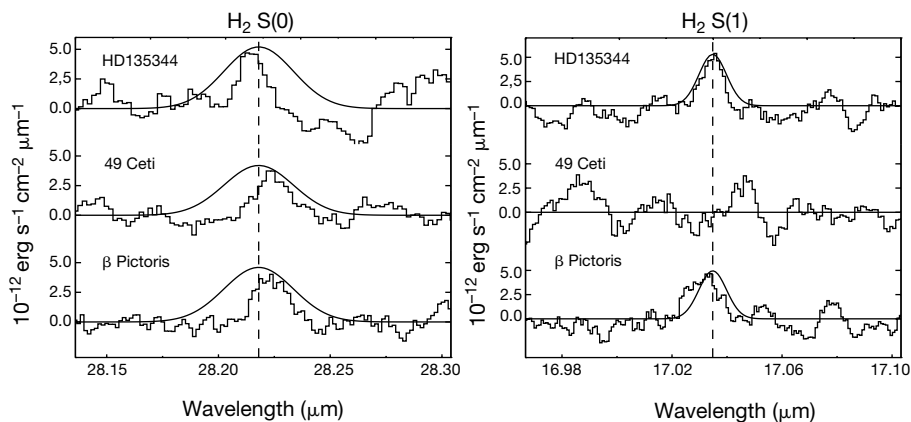


**Figure 1** Spectra of the lowest pure rotational molecular hydrogen transitions toward the  $\beta$  Pictoris, 49 Ceti, and HD135344 debris disks taken with the Infrared Space Observatory. The SWS mode 2 was used<sup>10</sup>, with an aperture of  $20'' \times 27''$  at the S(0) line and  $14'' \times 27''$  at the S(1) transition, corresponding to 400 AU  $\times$  540 AU and 280 AU  $\times$  540 AU, respectively, at the distance of  $\beta$  Pictoris (1 AU = Sun–Earth distance =  $1.5 \times 10^{13}$  cm). The dashed vertical line depicts the rest wavelengths of the  $H_2$  transitions, and the solid curve illustrates the range of potential wavelength shifts induced by grating repositioning errors or pointing offsets of the spacecraft. All line shapes

are consistent with the instrumental spectral resolution of  $\lambda/\Delta\lambda \approx 2,000/2,400$  at 28.218/17.035  $\mu\text{m}$ . Typical integration times were 600–1,000 s per line, in which the 12 SWS detectors were scanned several times over the 28.05–28.40 and 16.96–17.11  $\mu\text{m}$  intervals around the  $H_2$  lines. Individual scans are examined for cosmic ray glitches, dark current drifts, and readout non-linearities before being summed to produce a final spectrum<sup>12,14</sup>. Off-source integrations toward 49 Ceti and HD135344 reveal no  $H_2$  S(1) emission to a limiting flux of  $8 \times 10^{-15}$  ergs  $\text{s}^{-1} \text{ cm}^{-2}$  root mean square.

approximately the interstellar gas-to-dust ratio<sup>9</sup> of 100, but the total mass is below that of the so-called minimum mass solar nebula required to generate our own planetary system,  $\sim 10M_J$ . The  $H_2$  gas provides a reservoir from which gaseous giant planets may form, but, except for HD135344, the gas masses are insufficient to form any new Jupiter-mass planets in these optically thin disks. Indeed, provided the ages of these systems can be well constrained, such molecular hydrogen observations provide direct upper bounds for the formation timescales of jovian planets.

The presence of  $H_2$  but absence of CO can be understood from models of the photodestruction of these molecules in disks<sup>16</sup>. The ultraviolet radiation from the star and from the ambient interstellar radiation field can destroy CO in tenuous disks and in the outer layers of more massive disks, whereas freeze-out of the molecule onto the surfaces of grains<sup>17</sup> occurs in the cold inner part of massive disks. In contrast,  $H_2$  is not significantly removed by photolysis until the disk mass falls below  $10^{-3}M_J$ , and it does not freeze out onto grains. Millimetre-wave studies of both 49 Ceti and HD135344 have detected weak CO rotational line emission<sup>7,12</sup> consistent with gas gravitationally bound to the star, but the inferred molecular gas abundances are factors of 100–1,000 lower than found here. This has led to the perception that these and other ‘debris’ disks are largely free of gas, but our  $H_2$  observations indicate that this is not the case. The mechanisms through which the original massive disks were dissipated remain uncertain. Presumably, this involves a combination of accretion of matter inward onto the star and removal through interaction with a stellar wind and photo-evaporation, if the ultraviolet radiation from the star is sufficiently powerful<sup>18</sup>.

It has been postulated that various transitory optical features observed toward  $\beta$  Pictoris result from the evaporation of infalling planetesimals<sup>19,20</sup>, induced by dynamically important companions. It is difficult, however, to envision the required  $H_2$  mass being generated by secondary processes after disk dissipation. Furthermore, the high gas/dust ratios can significantly alter the dust transport dynamics. For disks with a negative radial pressure gradient, gas surface densities some 100–1,000 times lower than those originally present enlarge the grain size for which rapid outward drift occurs to diameters of  $\leq 100 \mu\text{m}$ , owing to the non-Keplerian velocity field of the gas and the co-rotation of the gas and dust<sup>21</sup>. Larger particles drift inward. If the gas mass is sufficiently large, dust generation by collisional cascade can be shut off completely even in optically thin disks<sup>22</sup>.

For  $\beta$  Pictoris, the low gas mass enhances the need for the *in situ* generation of 1–100  $\mu\text{m}$  dust grains<sup>23</sup>, because such particles can be efficiently ejected from the system; the gas/dust ratio of  $\sim 100$  found for  $\beta$  Pictoris could thus be coincidental in that substantial amounts of dust and gas may be hidden in large bodies. The gas masses derived for HD135344 and, perhaps, 49 Ceti may be large enough to prevent a collisional cascade of dust generation, yet increase the importance of radiative dust ejection, provided the disks are

optically thin. As such, they may be better interpreted as tenuous remnants of substantially more massive accretion disks. If so, HD135344 and 49 Ceti could be extremely interesting transition objects in which jovian planet formation may no longer be possible but for which the residual gas allows us to image gravitational perturbations in the disks owing to existing planets formed at earlier stages.

Central to this argument are the likely ages of the star/disk systems. For early-type field stars, the isochrones that are used to estimate ages based on stellar properties such as luminosity and effective temperature are consistent with two solutions. Vega, for example, can be interpreted either as a pre-main-sequence object a few Myr old or a main-sequence star whose age is  $\geq 300$  Myr. In most debris-disk studies, it is this older age that has been assumed<sup>4,5</sup>. The older ages lead to the natural conclusion that the dust must be regenerated *in situ*, because radiation pressure and Poynting–Robertson drag forces provoke the loss of less than micrometre-sized grains within only 0.1–1 Myr in gas-free disks, and also that dust disks are the most observable features of planetary systems like our own.

The age of  $\beta$  Pictoris has recently been estimated to be  $20 \pm 10$  Myr using nearby M dwarfs argued to be part of the same loose cluster on the basis of proper motion studies and *Hipparcos* distances<sup>24</sup>. Ages for 49 Ceti and HD135344 derived by recent pre-main-sequence stellar evolution models<sup>25</sup> are 8 and 17 Myrs, respectively, as shown in Table 1. In addition, HD135344 possesses certain features reminiscent of young Herbig Ae stars<sup>26</sup>. Thus, these objects may in fact be the descendants of circumstellar disks formed in a recent episode of local star formation.

Older stellar ages are consistent with the prevailing view that the probability of stars with ages of less than 10–30 Myr lying within a few tens of parsecs to the Sun is unlikely. The discovery of four nearby ( $d < 50$ –60 pc) young associations suggests, however, that local star formation happened as recently as 10–50 Myr ago, and that the Sun now lies within this stream of young stars<sup>27</sup>. For example, the G2 star/disk system HD207129 lies at a similar distance, as does  $\beta$  Pictoris, and has alternatively been assumed to be either 4.7 Gyr old<sup>28</sup> or only a few tens of millions of years in age<sup>27</sup>. Indeed, the sensitivity limitations of the IRAS all-sky survey that is the basis for most debris-disk searches and the ISO instruments used for follow-up ensured that only nearby or fairly massive disks have been located until now<sup>3,29</sup>. Searches for  $H_2$  such as that performed here can help to establish the gas/dust mass and evolutionary state of the sources, but only a small number of objects have been surveyed so far with adequate sensitivity. Our current understanding of remnant and debris disks may therefore be biased by the local star formation history and instrumental sensitivity. The present results suggest that jovian planet formation can occur on timescales of up to 20 Myr, but we stress the limited nature of the present sample. More massive disks easily capable of jovian planet formation are seen around several T Tauri and Herbig Ae stars of

**Table 1 Infrared Space Observatory  $H_2$  observations of debris disks**

Source	$d$ (pc)	Age (Myr)	$H_2$ S(0)	$H_2$ S(1)	$T_{\text{ex}}$ (K)	$H_2$ mass ( $M_J$ )	Dust mass ( $10^{-2} M_J$ )	$M_{H_2}$ via CO ( $M_J$ )
$\beta$ Pictoris	19.3	$20 \pm 10$	7.0	7.7	109	0.17	0.3	$< 6 \times 10^{-5}$
49 Ceti	61	$8 \pm 4$	6.6	$< 3$	$< 100$	$> 0.35$	0.63	0.006
HD135344	80	$17 \pm 3$	9.0	5.5	97	6.6	8.5	0.005

The integrated molecular hydrogen rotational line intensities, gas masses and dust masses toward the  $\beta$  Pictoris, 49 Ceti, and HD135344 debris disks. The integrated intensities of the  $H_2 J = 2 \rightarrow 0$  [S(0)] and  $J = 3 \rightarrow 1$  [S(1)] lines at 28.218 and 17.035  $\mu\text{m}$  are presented in units of  $10^{-14}$  ergs  $\text{s}^{-1}$   $\text{cm}^{-2}$ . Masses (in  $M_J$ ) are derived using local thermodynamic equilibrium (LTE) from the expression

$$M_{H_2} = 1.76 \cdot 10^{-17} \frac{F_{ul} d^2}{(hc/4\pi\lambda) A_{ul} x_u}$$

where  $d$  is the distance in parsec,  $F_{ul}$  is the flux of either the S(0) or S(1)  $H_2$  transition,  $h$  is Planck's constant,  $c$  is the speed of light,  $\lambda$  the observing wavelength, and  $A_{ul}$  is the Einstein spontaneous emission coefficient. The upper state population  $x_u$  for the line in question is very sensitive to the excitation temperature, which is fitted from the S(1)/S(0) ratio assuming that the ortho/para ratio is in LTE at the excitation temperature  $T_{\text{ex}}$  (ortho/para = 1.6 for  $T_{\text{ex}} = 100$  K). Numerically,  $T_{\text{ex}} = 505.24/\ln[1.12 \cdot 51 \cdot \text{S}(0)/\text{S}(1)]$ , in K. As upper limits only are available for the S(1) flux from 49 Ceti, the  $H_2$  mass is calculated for the upper temperature limit of 100 K, resulting in a lower bound for the mass. Dust masses are from the ISO measurements of ref. 15. The  $H_2$  mass for  $\beta$  Pictoris refers to the inner 400  $\text{AU}$ , which contains at least 80% of the disk mass<sup>16</sup>. The age estimates for 49 Ceti and HD135344 are derived using the pre-main-sequence stellar evolution tracks of ref. 25, and that for  $\beta$  Pictoris is taken from ref. 24. The main-sequence upper limit to the age of  $\beta$  Pictoris is approximately 100 Myr; the limits for 49 Ceti and HD135344 are even younger.

only slightly younger ages, for example, and illustrate the pressing need for better statistics<sup>12</sup>.

The Space Infrared Telescope Facility (SIRTF) to be launched by NASA in 2002 will go much deeper than IRAS and ISO, and will provide hundreds of new targets for further study. Improved molecular-line observations will also become possible with the high-resolution mid-infrared spectrometers nearing completion for use on large ground-based telescopes (for the 17- $\mu\text{m}$  S(1) line) and the Stratospheric Observatory for Infrared Astronomy (SOFIA) (for all H<sub>2</sub> lines including the 28- $\mu\text{m}$  S(0) transition). These diffraction-limited spectrometers will possess both the spatial and spectral resolution required to examine whether the gas and dust are co-spatial in the disks, and can establish whether the gas persists to within a few AU of the central star without the use of coronagraphic techniques. In the longer term, a mid-infrared spectrometer on the Next Generation Space Telescope (NGST) would make possible the detection of Earth-masses of H<sub>2</sub> gas at temperatures down to 50 K. By combining continuum and line studies of disks around stars up to several tens of Myr in age, it will be possible to determine both gas/dust dissipation and jovian planet formation timescales; and to examine the role of collisional, radiative and gaseous processes in shaping the evolution and survival of dust clouds in planetary systems. □

Received 25 September 2000; accepted 16 November 2000.

1. Beckwith, S. W. V. & Sargent, A. I. Circumstellar disks and the search for neighbouring planetary systems. *Nature* **383**, 139–144 (1996).
2. Aumann, H. *et al.* Discovery of a shell around Alpha Lyrae. *Astrophys. J.* **278**, L23–L27 (1984).
3. Backman, D. E. & Paresce, F. in *Protostars & Planets III* (eds Levy, E. H. & Lunine, J. I.) 1253–1304 (Univ. Arizona Press, Tucson, 1993).
4. Habing, H. J. *et al.* Disappearance of stellar debris disks around main-sequence stars after 400 million years. *Nature* **401**, 456–458 (1999).
5. Lagrange, A. M., Backman, D. E. & Artymowicz, P. in *Protostars & Planets IV* (eds Mannings, V., Boss, A. & Russell, S.) 639–672 (Univ. Arizona Press, Tucson, 2000).
6. Greaves, J. S., Coulson, I. M. & Holland, W. S. No molecular gas around nearby solar-type stars. *Mon. Not. R. Astron. Soc.* **312**, L1–L3 (2000).
7. Zuckerman, B., Forveille, T. & Kastner, J. H. Inhibition of giant planet formation by rapid gas depletion around young stars. *Nature* **373**, 494–496 (1995).
8. Dent, W. R. F., Greaves, J. S., Mannings, V., Coulson, I. M. & Walther, D. M. A search for molecular gas components in prototypical Vega-excess systems. *Mon. Not. R. Astron. Soc.* **277**, L25–L29 (1995).
9. Hildebrand, R. H. The determination of cloud masses and dust characteristics from submillimeter thermal emission. *Q. J. R. Astron. Soc.* **24**, 267–282 (1983).
10. de Graauw, T. *et al.* Observing with the ISO Short Wavelength Spectrometer. *Astron. Astrophys.* **315**, L49–L54 (1996).
11. Kessler, M. *et al.* The Infrared Space Observatory (ISO) mission. *Astron. Astrophys.* **315**, L64–L70 (1996).
12. Thi, W. F. *et al.* H<sub>2</sub> and CO emission from disks around T Tauri, Herbig Ae and Vega-type stars: cold and warm circumstellar gas. *Astrophys. J.* (submitted).
13. Thi, W. F., van Dishoeck, E. F., Blake, G. A., van Zadelhoff, G. J. & Hogerheijde, M. R. Detection of H<sub>2</sub> pure rotational line emission from the GG Tau circumbinary disk. *Astrophys. J.* **521**, L63–L66 (1999).
14. Valentijn, E. A. & Thi, W. F. ISO's Short Wavelength Spectrometer—Ultimate sensitivity. Reducing the effects of cosmic weather. *Exp. Astron.* **10**, 215–225 (2000).
15. Walker, H. J. & Heinrichsen, I. ISOPHOT observations of dust disks around main-sequence (Vega-like) stars. *Icarus* **143**, 147–154 (2000).
16. Kamp, I. & Bertoldi, F. CO in the circumstellar disks of Vega and  $\beta$  Pictoris. *Astron. Astrophys.* **353**, 276–286 (2000).
17. Sandford, S. A. & Allamandola, L. J. H<sub>2</sub> in interstellar and extragalactic ices—Infrared characteristics, ultraviolet production, and implications. *Astrophys. J.* **409**, L65–L68 (1993).
18. Hollenbach, D. J., Yorke, H. W. & Johnstone, D. in *Protostars & Planets IV* (eds Mannings, V., Boss, A. & Russell, S.) 401–428 (Univ. Arizona Press, Tucson, 2000).
19. Lagrange, A. M. *et al.* The  $\beta$  Pic circumstellar disk. XXIV. Clues to the origin of the stable gas. *Astron. Astrophys.* **310**, 1091–1108 (1998).
20. Heap, S. R. *et al.* STIS coronagraphic observations of  $\beta$  Pictoris. *Astrophys. J.* **539**, 435–444 (2000).
21. Klahr, H. H. & Lin, D. N. C. Dust distribution in gas disks. A model for the ring around HR 4796A. *Astron. J.* (in the press).
22. Weidenschilling, S. J. Aerodynamics of solid bodies in the solar nebula. *Mon. Not. R. Astron. Soc.* **180**, 57–70 (1977).
23. Artymowicz, P. & Clampin, M. Dust around main sequence stars: Nature or nurture by the interstellar medium? *Astrophys. J.* **490**, 863–878 (1997).
24. Barrado y Navascués, D., Stauffer, J. R., Song, I. & Cailleault, J. P. The age of  $\beta$  Pictoris. *Astrophys. J.* **520**, L123–L126 (1999).
25. Siess, L., Forestini, M. & Bertout, C. Physics of accretion onto young stars. III. Comparisons with observations. *Astron. Astrophys.* **342**, 480–491 (1999).
26. Dunkin, S. K., Barlow, M. J. & Ryan, S. G. High-resolution spectroscopy of Vega-like stars—II. Age indicators, activity and circumstellar gas. *Mon. Not. R. Astron. Soc.* **290**, 165–185 (1997).
27. Zuckerman, B. & Webb, R. A. Identification of a nearby stellar association with the *Hipparcos* catalog: Implications for recent, local star formation. *Astrophys. J.* **535**, 959–964 (2000).
28. Jourdain de Muizon, M., Laureijs, R. J., Dominik, C. & Habing, H. J. A very cold disk of dust around the G2V star HD 207129. *Astron. Astrophys.* **350**, 875–882 (1999).

29. Fajardo-Acosta, S. B., Stencel, R. E., Backman, D. E. & Thakur, N. Infrared Space Observatory photometric search of main-sequence stars for Vega-type Systems. *Astrophys. J.* **520**, 215–222 (1999).

**Acknowledgements**

This work was supported by The Netherlands Organization for Scientific Research (NWO). Additional support to G.A.B. from the NASA Infrared Space Observatory (ISO), Exobiology, and Origins of Solar Systems programmes is gratefully acknowledged. A.N. is supported in part by an Agenzia Spaziale Italiana (ASI) grant. This work is based on observations with ISO, a European Space Agency (ESA) project with instruments funded by ESA Member States (especially the Principal Investigator countries: France, Germany, the Netherlands, and the United Kingdom) and with the participation of the Institute of Space and Astronautical Sciences (ISAS) and the National Aeronautics and Space Administration (NASA).

Correspondence should be addressed to G.A.B. (e-mail: gab@gps.caltech.edu).

.....  
**Many-particle entanglement with Bose–Einstein condensates**

**A. Sørensen\*, L.-M. Duan†, J. I. Cirac† & P. Zoller†**

\* *Institute of Physics and Astronomy, University of Aarhus, DK-8000 Århus C, Denmark*

† *Institute for Theoretical Physics, University of Innsbruck, A-6020 Innsbruck, Austria*

.....  
**The possibility of creating and manipulating entangled states of systems of many particles is of significant interest for quantum information processing; such a capability could lead to new applications that rely on the basic principles of quantum mechanics<sup>1</sup>. So far, up to four atoms have been entangled in a controlled way<sup>2,3</sup>. A crucial requirement for the production of entangled states is that they can be considered pure at the single-particle level. Bose–Einstein condensates<sup>4–6</sup> fulfil this requirement; hence it is natural to investigate whether they can also be used in some applications of quantum information. Here we propose a method to achieve substantial entanglement of a large number of atoms in a Bose–Einstein condensate. A single resonant laser pulse is applied to all the atoms in the condensate, which is then allowed to evolve freely; in this latter stage, collisional interactions produce entanglement between the atoms. The technique should be realizable with present technology.**

Consider a set of  $N$  two-level atoms confined by some external trap. In order to describe the internal properties of these atoms, it is convenient to let the internal states  $|a\rangle_n$  and  $|b\rangle_n$  of the  $n$ th atom represent the two states of a fictitious spin-1/2 particle with angular momentum operators  $j_x^{(n)} = 1/2(|a\rangle\langle a|_n - |b\rangle\langle b|_n)$ ,  $j_y^{(n)} = 1/2(|b\rangle\langle a|_n + |a\rangle\langle b|_n)$ , and  $j_z^{(n)} = i/2(|b\rangle\langle a|_n - |a\rangle\langle b|_n)$ . We consider collective effects of the atoms that are described by total angular momentum operators,  $\mathbf{J} = \sum_{n=1}^N \mathbf{j}^{(n)}$ . The entanglement properties of the atoms can be expressed in terms of the variances and expectation values of these operators. In the Methods section we show that if

$$\xi^2 \equiv \frac{N(\Delta J_{n_1})^2}{\langle J_{n_2} \rangle^2 + \langle J_{n_3} \rangle^2} < 1 \tag{1}$$

where  $J_n \equiv \mathbf{n} \cdot \mathbf{J}$  and the  $\mathbf{n}$ s are mutually orthogonal unit vectors, then the state of the atoms is non-separable (that is, entangled). The parameter  $\xi^2$  thus characterizes the atomic entanglement, and states with  $\xi^2 < 1$  are often referred to as “spin squeezed states”<sup>7</sup>. Here we show how to reduce  $\xi^2$  by several orders of magnitude using the collisional interactions between atoms in a Bose–Einstein condensate.